

# Optimization of PVC– PAN-Based Polymer Electrolytes

Somasundaram Rajendran,<sup>1</sup> Ravishanker Babu,<sup>1</sup> Periyasami Sivakumar<sup>2</sup>

<sup>1</sup>Department of Physics, Alagappa University, Karaikudi, Tamilnadu, India

<sup>2</sup>Department of Physics, H.H. The Rajah's College, Pudukottai, Tamilnadu, India

Received 17 July 2006; accepted 15 May 2007

DOI 10.1002/app.30174

Published online 17 April 2009 in Wiley InterScience (www.interscience.wiley.com).

**ABSTRACT:** The hybrid plasticized polymer electrolyte composed of the blend of poly(vinyl chloride) (PVC) and poly(acrylonitrile) (PAN) as host polymer, propylene carbonate as plasticizer, and LiClO<sub>4</sub> as a salt was studied. An attempt was made to optimize the polymer blend ratio. XRD, Fourier transform infrared, and DSC studies confirm the formation of polymer–salt complex and miscibility of

the PVC and PAN. The electrical conductivity and temperature dependence of ionic conductivity of polymer films are also studied and reported here. © 2009 Wiley Periodicals, Inc. *J Appl Polym Sci* 113: 1651–1656, 2009

**Key words:** PVC/PAN polymer blend electrolytes; XRD; FTIR and impedance studies

## INTRODUCTION

In recent years, there has been an increasing need for rechargeable batteries of high specific energy for portable electronic equipment. Among them the lithium-polymer batteries are now widely being investigated and developed because these batteries can be produced in a variety of forms, permitting production of portable batteries possessing required shape and enabling customization of portable-power electronic equipment.<sup>1–3</sup> Conventional poly(ethylene oxide)-based polymer electrolytes pioneered by Wright and coworkers,<sup>4,5</sup> and followed by Armand et al.<sup>6</sup> are the most commonly studied. These electrolytes exhibit conductivities ranging from 10<sup>−8</sup> to 10<sup>−5</sup> S cm<sup>−1</sup> at room temperature, which preclude their practical applications.<sup>7</sup>

Investigations were focused fervently on the enhancement of conductivity at room temperature via various approaches, such as blending of polymers,<sup>8</sup> cross-linking,<sup>9</sup> insertion of ceramic fillers,<sup>10</sup> plasticization,<sup>11</sup> etc. The repercussions of these are reduction in crystallinity of the polymer or lowering of the glass transition temperature ( $T_g$ ). It is generally observed, however, that high ionic conductivity is achieved at the expense of good dimensional stability.<sup>12</sup> Of the said techniques, blending of polymers is a fabulous method to develop new materials with improved mechanical stability. In 1975,<sup>13,14</sup> the concept of gel polymer electrolytes came into existence. These electrolytes had liquid electrolyte immobilized in polymer matrix and exhibit ionic conductivity in

excess of 10<sup>−3</sup> S cm<sup>−1</sup> at room temperature. The mechanical properties are not sufficient, however, to produce thin films, because the impregnation of a liquid electrolyte into a polymer results in softening of the polymer. For these plasticized electrolytes, poly(vinylidene fluoride) (PVdF),<sup>15</sup> poly(acrylonitrile) (PAN),<sup>16–18</sup> poly(methyl methacrylate) (PMMA),<sup>19</sup> poly(vinyl chloride) (PVC),<sup>20</sup> and the blend systems based on poly(ethylene oxide) (PEO),<sup>21–23</sup> have been used as host polymers.

PAN, one of the host polymers used in the plasticized polymer electrolyte, was first reported by Reich and Micaeli<sup>24</sup> and followed by Watanabe et al.,<sup>25</sup> Abraham and Alamgir.<sup>26</sup> The PAN-based plasticized polymer electrolyte indubitably showed conductivity of the order 10<sup>−3</sup> S cm<sup>−1</sup> with PC, ethylene carbonate (EC) mixture as plasticizers and LiClO<sub>4</sub> in PAN, despite its high conductance, dimensional stability of these films were not noteworthy because of the existence of a liquid solution entrapped in the PAN matrix. However, these electrolytes suffer from a gel-like mechanical property; it does not form free-standing film at high plasticizer content. For that reason, an improvement in mechanical property of the PAN-based plasticized electrolyte is required for materialization.

The proof of the blend concept was demonstrated with PVC/PMMA polymer electrolyte by Roo et al.<sup>27</sup> and the characterization of a lithium-ion polymer battery that used PVC/PMMA polymer electrolyte was reported by Kim et al.<sup>28</sup> In the current article, we have studied the new plasticized polymer electrolyte comprising PVC/PAN blend as host polymer, propylene carbonate (PC) as plasticizer, and LiClO<sub>4</sub> as a salt. PVC is incorporated into the plasticized PAN system to circumvent the drawback

Correspondence to: S. Rajendran (sraj54@yahoo.com).

inherent to plasticization of PAN, i.e., poor mechanical property. Because of the immiscibility of PVC with the plasticizer, the electrolyte film has a phase-separated morphology consisting of PVC-rich phase and the other. The plasticizer-rich phase with PAN will provide a pathway for the ionic conduction and the PVC-rich phase acts as a mechanical stiffener for the electrolyte films.<sup>29,30</sup> We have attempted to investigate the complexation through X-ray diffraction (XRD) and Fourier transform infrared (FTIR) studies, miscibility by differential scanning calorimetry (DSC) analysis, and conductivity by ac impedance spectroscopy.

### EXPERIMENTAL

The electrolytes were prepared from polymers PVC (average molecular weight  $1.5 \times 10^5$ ) and PAN (average molecular weight 94,000), plasticizer PC, and the inorganic salt  $\text{LiClO}_4$  purchased from Aldrich, USA. To obtain the homogeneous films, further purification of components is essential. The polymers were dried under vacuum of about  $10^{-3}$  torr at temperature well above the glass transition temperature and below their melting temperature for about 12 h. The inorganic salt  $\text{LiClO}_4$  was annealed at  $100^\circ\text{C}$  and the plasticizer PC was used as such without further purification. For vacuum drying Logitech DTC 5050 vacuum oven was used.

The corresponding weights of PVC, PAN, and  $\text{LiClO}_4$  were dissolved in distilled di-methyl formamide (DMF). The solutions thus obtained were mixed and stirred continuously for 48 h at  $30^\circ\text{C}$  and then at  $70^\circ\text{C}$  until a homogeneous gelly nature was obtained. The obtained suspension was cast on to glass plates and Teflon bushes. DMF was allowed to evaporate slowly and then the film was dried at  $60^\circ\text{C}$  in a vacuum oven to remove traces of DMF present.

The resulting film was visually examined for its dryness and free-standing nature. Chemical storage, film casting, and cell assemblies were performed in the vacuum atmosphere. Thickness of the film was found to be from 0.1 to 0.3 mm.

The XRD equipment used in this study was JEOL JDX 8030 X-ray diffractometer with Ni-filtered  $\text{CuK}_\alpha$  radiation ( $\beta = 1.541\text{\AA}$ )  $\theta - 2\theta$  coupling mode. FTIR measurements were made in the range  $4000\text{--}400\text{ cm}^{-1}$  using Perkin Elmer Paragon IR spectrophotometer model (577). The electrical conductivity measurements have been performed by using complex ac impedance technique. The bulk electrical conductivity of the polymer films was evaluated from the impedance plots. Also, the plots were recorded in the range 40 Hz to 100 kHz with signal amplitude of 10 mV using Keithley 3330 LCZ meter. The polymer electrolyte film was sandwiched between stainless

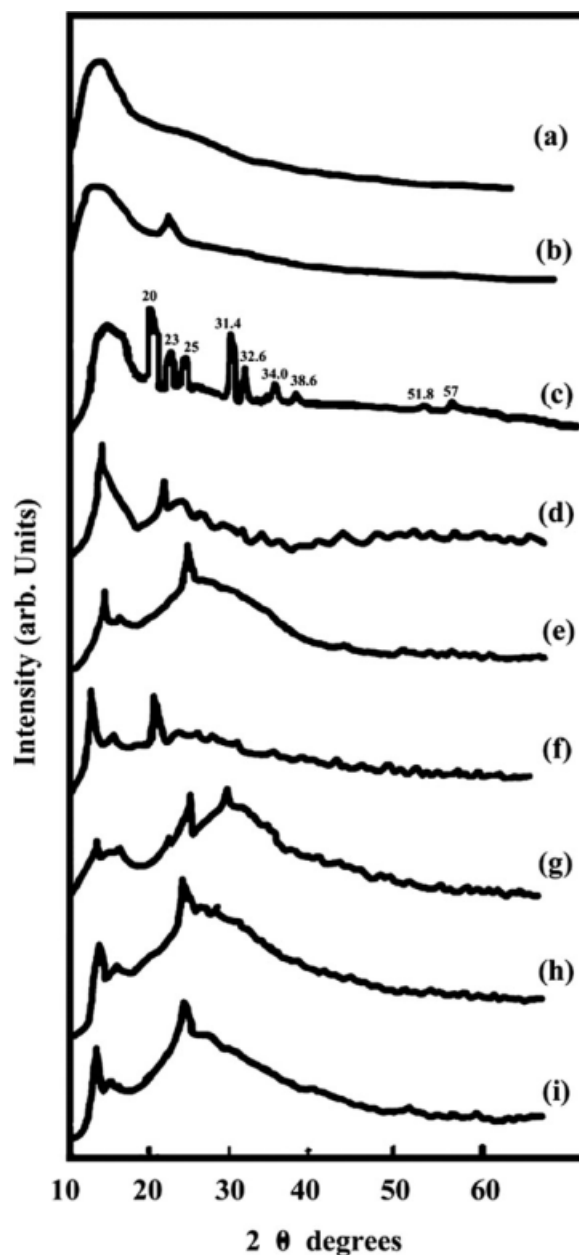


**Figure 1** X-ray diffraction patterns of (a) PVC (b) PAN (c)  $\text{LiClO}_4$  (d) PVC(30)–PAN(0)– $\text{LiClO}_4$ (8)–PC(62) (e) PVC(24)–PAN(6)– $\text{LiClO}_4$ (8)–PC(62) (f) PVC(18)–PAN(12)– $\text{LiClO}_4$ (8)–PC(62) (g) PVC(12)–PAN(18)– $\text{LiClO}_4$ (8)–PC(62) (h) PVC(6)–PAN(24)– $\text{LiClO}_4$ (8)–PC(62) (i) PVC(0)–PAN(30)– $\text{LiClO}_4$ (8)–PC(62).

steel electrodes attached to the conductivity jig specially designed and fabricated for this purpose.

### RESULTS AND DISCUSSION

#### XRD analysis

X-ray diffraction pattern of pure PVC, PAN,  $\text{LiClO}_4$ , and complexes are shown in Figure 1(a–i). The following observations are made

- Figure 1(d-i) shows the XRD diffractograms of PVC-PAN-LiClO<sub>4</sub>-PC complexes. Figure 1(d) shows the XRD spectrum of PVC-LiClO<sub>4</sub>-PC complex. Figure 1(e-i) shows the chronological increase in amorphicity as the concentration of PAN is increased in the complexes. The highest amorphicity is seen for the film bereft of PVC (i.e., film with PAN-LiClO<sub>4</sub>-PC), which shows highest conductivity but poor mechanical stability. When compared with other complexes, the film containing the next higher amorphicity, conductivity with good mechanical stability is obtained for film consisting of PVC(6)-PAN(24)-LiClO<sub>4</sub>-PC(62) [shown in Fig. 1 (h)] ratio. Hence, it is concluded that 6 : 24 : 8 : 62 (PVC-PAN-LiClO<sub>4</sub>-PC) composition would have provided proper blending of polymers.
- The sharp crystalline peaks of LiClO<sub>4</sub> [Figure 1(c)] are found to be absent in the complexes, which indicates the complete dissolution of lithium salts in the polymer matrices.

The XRD studies confirmed the fact that there exist a definite complex coordination between PVC, PAN, LiClO<sub>4</sub>, and PC.

### FTIR studies

FTIR is an appropriate method for monitoring the coordination of Li-ion, complex formation, etc. Complexation may shift in the cage peak frequencies. The FTIR of pure PVC, PAN, LiClO<sub>4</sub>, PC, and polymer complexes are shown in Figure 2(a-j). The band at 612 cm<sup>-1</sup> assigned to  $\gamma$ (C-Cl) stretching of PVC is shifted in all the complexes containing PVC, the trans CH<sub>2</sub> wagging of PVC at 966 cm<sup>-1</sup> is shifted around 956 cm<sup>-1</sup> and the intensity is found to decrease with the increase of PAN content. The vibrational bands at 1254 cm<sup>-1</sup> and 1250 cm<sup>-1</sup> assigned to CH rocking and C-N stretching of PVC and PAN, respectively, are found to be shifted to an intermediate frequency at 1252 cm<sup>-1</sup> in all the complexes, except those of pure PVC-LiClO<sub>4</sub>-PC and PAN-LiClO<sub>4</sub>-PC. This may be due to the interaction between the PAN and PVC molecules. The CH<sub>2</sub> deformation frequency at 1333 cm<sup>-1</sup> is found to be shifted slightly in all the complexes except the system bereft of PVC in which this frequency is absent. The asymmetrical CH<sub>2</sub> stretching of PAN at 2942 cm<sup>-1</sup> is found to be shifted in all the complexes containing PAN. The C≡N stretching frequency at 2245 cm<sup>-1</sup> of PAN is found to be shifted in all the complexes and this may be attributed to the interaction of PAN with salt and the plasticizer.<sup>31</sup>

Apart from the shift in frequencies, there are a few peaks found absent and some new peaks present in the complexes. The vibrational bands at (2913,

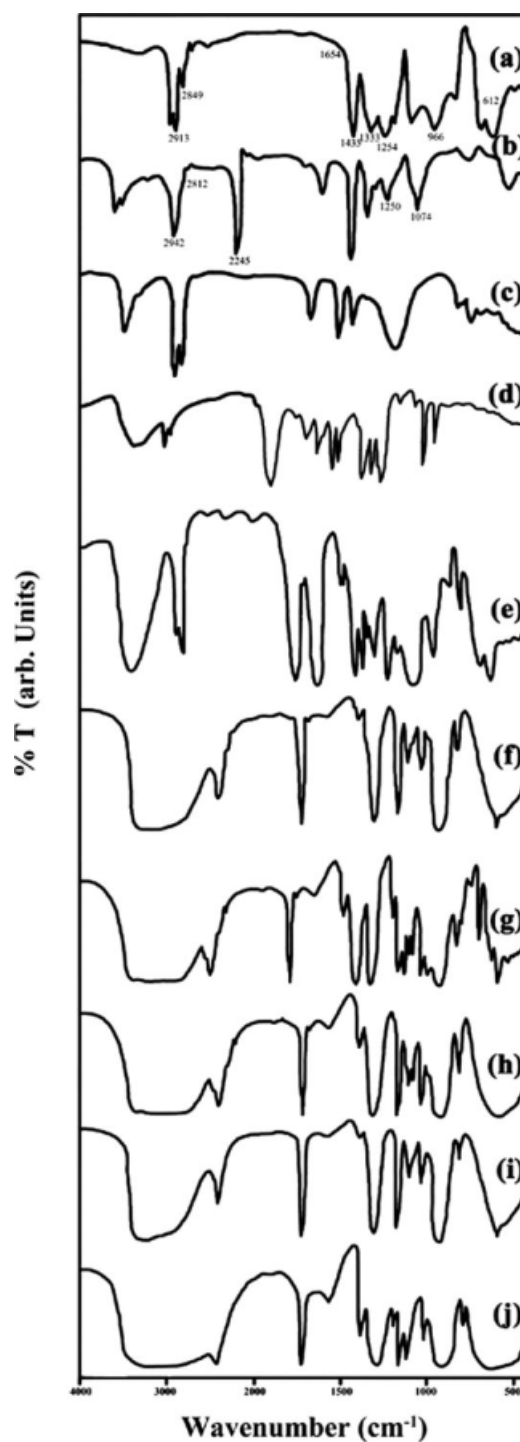


**Figure 2** FTIR spectra of (a) PVC, (b) PAN, (c) (LiClO<sub>4</sub>), (d) PC, (e) PVC (30)-LiClO<sub>4</sub> (8)-PC (62), (f) PVC (24)-PAN (6)-LiClO<sub>4</sub> (8)-PC (62), (g) PVC (18)-PAN (12)-LiClO<sub>4</sub> (8)-PC (62), (h) PVC (12)-PAN (18)-LiClO<sub>4</sub> (8)-PC (62), (i) PVC (6)-PAN (24)-LiClO<sub>4</sub> (8)-PC (62), and (j) PAN (30)-LiClO<sub>4</sub> (8)-PC (62).

2849, 1654, and 1435) assigned to asymmetrical CH<sub>2</sub> stretching, symmetrical CH<sub>2</sub> stretching, C=C stretching, and CH<sub>2</sub> bending of PVC, (2812 and 1074 cm<sup>-1</sup>) assigned to CH<sub>2</sub> stretching, C-C stretching of PAN, (1186, 1097, 712, and 555 cm<sup>-1</sup>) of LiClO<sub>4</sub> and

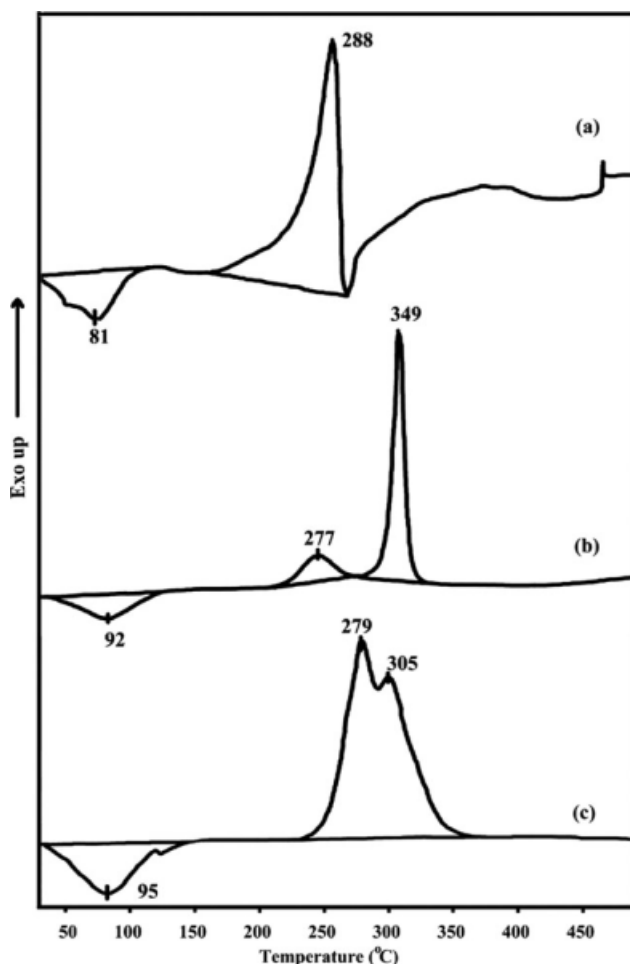


**Figure 3** DSC spectra of (a) PVC(30)-LiClO<sub>4</sub>(8)-PC(62), (b) PAN(30)-LiClO<sub>4</sub>(8)-PC(62), and (c) PVC(6)-PAN(24)-LiClO<sub>4</sub>(8)-PC(62).

(2358, 1340, 1121, 849, and 534 cm<sup>-1</sup>) of PC are found absent and the following new bands are found to be present (3560, 1774, 1650, 1454, 1108, and 406 cm<sup>-1</sup>) in all the complexes. The above analysis establishes the formation of polymer salt complexes.<sup>27,32-37</sup>

### DSC studies

The DSC data of the systems containing pure PVC-LiClO<sub>4</sub>-PC, PAN-LiClO<sub>4</sub>-PC and the complex PVC-PAN-LiClO<sub>4</sub>-PC, which gives the maximum conductivity and good mechanical stability is shown in Figure 3(a-c), respectively. The original glass transition temperature of PVC and PAN are 81 and 92°C, respectively. In Fig. 3(a,b), the endothermic peak at 86 and 95°C corresponds to the glass transition temperature ( $T_g$ ) of PVC and PAN, which are complexed with LiClO<sub>4</sub> and PC individually. This marginal shift in  $T_g$  of polymer salt complex to a higher side may be due to the addition of lithium salt.<sup>38</sup> In Figure 3(a), an exothermic peak observed

in the range 180–300 °C may be attributed to the melting of the crystallites in the vicinity of the atactic phase of PVC. The crystalline temperature  $T_c$  is observed at 288°C. In Figure 3(b), two exothermic peaks in the range 240–280 °C and 310–380 °C with a peak maximum at 277 and 349°C, respectively, are observed. These two peaks observed at 277 and 349°C could be attributed to crystallization temperature of PC and PAN, respectively. This crystallization temperature is particularly seen in Figure 3(b) due to the entrapped plasticizer (PC) by PAN. This peak is not visible in Figure 3(a) because of the tendency of immiscibility of PAN with plasticizers. In Figure 3(c), an endothermic peak is observed at 82°C and an exothermic peak in the form of doublet in the range 230–380 °C corresponding to glass transition temperature and crystalline temperature, respectively. It is found that there is a single  $T_g$  and a combined  $T_c$  as observed in Figure 3(c). These two peaks at 279 and 305°C, which are the crystalline temperatures of PVC and PAN that would have shifted from its original [Fig. 3(a,b)] due to the complexation of the polymers. Hence, the confirmation of miscibility.

### Conductivity studies

Impedance spectroscopy is used to establish the conductivity mechanism, observing the participation of the polymer chain mobility and carrier generation process. The impedance studies of PVC/PAN blend electrolytes for different compositions were made. The ac impedance spectra of SS-SPE-SS (SPE: solid polymer electrolyte, SS: stainless steel) system with the highest conductivity and good mechanical stability is shown in Figure 4.

The conductivity of the polymer electrolyte was calculated from the measured resistance for the known area 'A' and thickness of the polymer film 'l'.

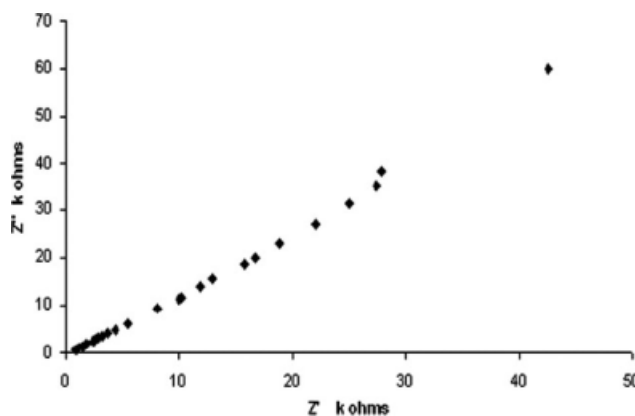


**Figure 4** The complex impedance plot of PVC (6)-PAN (24)-LiClO<sub>4</sub> (8)-PC (62) at 303 K.

TABLE I  
Conductivity Values of PVC-PAN-LiClO<sub>4</sub>-PC Polymer Complexes

Sample	Composition				Conductivity $\times 10^{-4}$ S cm <sup>-1</sup>					Condition
	PVC	PAN	LiClO <sub>4</sub>	PC	302 K	318 K	333 K	353 K	373 K	
A1	30	0	8	62	0.067	0.148	0.158	0.171	0.255	Brittle
A2	24	6	8	62	0.227	0.293	0.421	0.595	0.940	Free standing
A3	18	12	8	62	0.324	0.479	1.080	1.120	2.020	Free standing
A4	12	18	8	62	0.407	0.676	1.860	3.330	4.030	Free standing
A5	6	24	8	62	0.701	0.959	2.650	4.190	5.230	Free standing
A6	0	30	8	62	1.380	2.690	4.660	6.490	7.530	Gelly

The disappearance of semicircular portion in the impedance curve leads to a conclusion that the current carriers are ions and this leads one to further conclude that the total conductivity is mainly the result of ion conduction.<sup>39</sup>

The ionic conductivity was calculated using the relation  $\sigma = 1/R_b A$ , where  $R_b$  is the bulk resistance. Table I shows the conductivity values of the complex in the temperature range 303–373 K. The impedance diagram for the PAN-PVC-LiClO<sub>4</sub>-PC (film A5) is shown in Figure 4. The conductivity of this system is  $7.01 \times 10^{-5}$  S cm<sup>-1</sup> at 303 K, which has better dimensional stability. The data given in Table I show that the conductivity increases with the increase in temperature. This behavior can be rationalized by recognizing the free-volume model.<sup>34</sup> As the temperature increases, the polymer can expand easily and produce free volume. Thus, ions, solvated molecules, or polymer segments can move into the free volume.<sup>40</sup> The resulting conductivity represented by the overall mobility of ion and polymer is determined by the free-volume around the polymer chains. Therefore, as the temperature increases, the free volume increases. This leads to an increase in ion mobility and segmental mobility that will assist ion transport and virtually compensate for the retarding effect of the ion clouds.

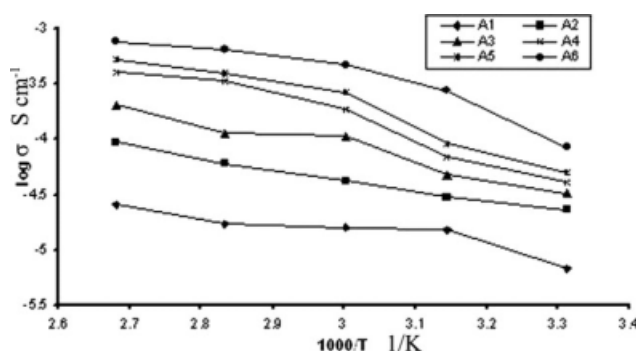


Figure 5 Arrhenius plot of log conductivity versus 1000/T for (A1) PVC(30)-PAN(0)-LiClO<sub>4</sub>(8)-PC(62), (A2) PVC(24)-PAN(6)-LiClO<sub>4</sub>(8)-PC(62), (A3) PVC(18)-PAN(12)-LiClO<sub>4</sub>(8)-PC(62), (A4) PVC(12)-PAN(18)-LiClO<sub>4</sub>(8)-PC(62), (A5) PVC(6)-PAN(24)-LiClO<sub>4</sub>(8)-PC(62), and (A6) PVC(0)-PAN(30)-LiClO<sub>4</sub>(8)-PC(62).

Figure 5 shows the Arrhenius plot of the ionic conductivity for all compositions given in Table I. The temperature dependence on the ionic conductivity is not linear, which suggest that the ion conduction follows the William-Landell-Ferry mechanism.<sup>41</sup> That is, ion transport in polymer electrolytes is correlated with polymer segmental motion.<sup>42</sup>

## CONCLUSION

Complex formation and miscibility of PVC-PAN-LiClO<sub>4</sub>-PC polymer complex has been confirmed from FTIR, XRD, and DSC studies. The film with the concentration PVC (6): PAN (24): LiClO<sub>4</sub> (8): PC (62) is optimized to have the highest ionic conductivity ( $7.01 \times 10^{-5}$  S cm<sup>-1</sup>) with good mechanical stability. The temperature dependence of ionic conductivity is explained on the basis of free volume model.

## References

- Mac Callum, J. R.; Vincent, C. A., Eds. *Polymer Electrolyte Reviews*; Elsevier: London, 1987–1989; Vols. 1 and 2.
- Lipkowski, J.; Ross, P. N., Eds. *The Electrochemistry of Novel Materials*; VCH: New York, 1994.
- Scrosati, B. *Applications of Electroactive Polymers*; Chapman & Hall: London.
- Gray, F. M. *Solid Polymer Electrolytes— Fundamentals and Technological Applications*; VCH: New York, 1991.
- Fenton, D. E.; Parker, J. M.; Wright, P. V. *Polymer* 1973, 14, 589.
- Armand, M. B.; Chabagno, J. M.; Duclot, M. J. In *Fast Ion Transport in Solids*, Duclot, M. J.; Vashista, P.; Mundy, J. M.; Shenoy, G. K., Eds., 1979.
- Gray, F. M. *Solid Polymer Electrolytes*; VCH: New York, 1991.
- Kim, D. W.; Park, J. R.; Rhee, H. W. *Solid State Ion* 1996, 83, 49.
- Wieckzorek, W.; Stevans, J. R. *J Phys Chem B* 1997, 101, 1529.
- Przyluski, J.; Wieckzorek, W. *Solid State Ion* 1989, 36, 165.
- Cherng, J. Y.; Munshi, M. Z. A.; Owens, B. B.; Smyrl, W. H. *Solid State Ion* 1988, 28, 857.
- Appetecchi, G. B.; Croce, F.; Scrosati, B. *Electrochim Acta* 1995, 40, 991.
- Feuillade, G.; Perch, P. *J Appl Electrochem* 1975, 5, 63.
- Abraham, K. M.; Alamgir, M. *J Electrochem Soc* 1990, 137, 1657.
- Tsuchida, E.; Ohno, H.; Tsunemi, K. *Electrochim Acta* 1983, 28, 591.
- Abraham, K. M.; Alamgir, M. United States Patent No., 1993.

17. Hong, H.; Liqun, C.; Xuejie, H.; Rongjian, X. *Electrochim Acta* 1992, 37, 1671.
18. Peramunage, D.; Pasquariello, D. M.; Abraham, K. M. *J Electrochem Soc* 1995, 142, 1789.
19. Bonhke, O.; Frand, G.; Rezzazi, M.; Rousselot, C.; Truche, C. *Solid State Ion* 1993, 66, 97.
20. Alamgir, M.; Abraham, K. M. *J Electrochem Soc* 1993, 140, L96.
21. Mani, T.; Stevens, J. R. *Polymer* 1992, 33, 834.
22. Lee, H. S.; Yang, X. Q.; Mc Breen, J. *J Electrochem Soc* 1994, 14, 886.
23. Walker, C. W., Jr; Salomon, M. *J Electrochem Soc* 1993, 140, 3409.
24. Reich, S.; Michaeli, I. *J Power Sources* 1995, 55, 7.
25. Watanabe, M.; Kanaba, M.; Matsuda, H.; Mizoguchi, K.; Tsuchida, E.; Tsunemi, K. *Makromol Chem Rapid Commun* 1981, 2, 741.
26. Abraham, K. M.; Alamgir, M. *J Electrochem Soc* 1990, 136, 1657.
27. Roo, H. J.; Kim, H. T.; Park, J. K. *Electrochim Acta* 1997, 42, 1571.
28. Kim, H. T.; Kim, K. B.; Kim, S. W.; Park, J. K. *Electrochim Acta* 2000, 45, 4001.
29. Manuel Stephen, A.; Thirunakaran, R.; Pitchumani, S.; Prem Kumar, T.; Muniyandi, N. *J Power Sources* 2000, 89, 80.
30. Manuel Stephen, A.; Thirunakaran, R.; Pitchumani, S.; Prem Kumar, T.; Muniyandi, N. *Solid State Ion* 2000, 130, 123.
31. Wang, Z.; Huang, B.; Wang, S.; Xue, R.; Huang, X.; Chen, L. *J Electrochem Soc* 1997, 144, 778.
32. Jacob, M. M. E.; Prabaharan, S. R. S.; Radhakrishnan, S. *Solid State Ion* 1997, 104, 267.
33. Armand, M. B.; Chabagno, J. M.; Duclot, M. J. In *Fast-Ion Transport in Solids*, Vashista, P.; Mundy, L. N.; Shenoy, G. K., Eds; North-Holland: Amsterdam, 1979, p 131.
34. Miya Molo, T.; Shibayana, K. *J Appl Phys* 1973, 44, 5372.
35. Vogel, H. *Phys Z* 1922, 22, 645.
36. Tamman, V. G.; Hesse, H. *Anorg Allg Chem* 1926, 19, 245.
37. Flucher, G. S. *J Am Ceram Soc* 1925, 8, 339.
38. Blonsky, P. M.; Shriver, D. F.; Austin, P.; Allock, H. R. *Solid State Ion* 1986, 18, 258.
39. Izuchi, S.; Ochiai, S.; Takeuchi, K. *J Power Sources* 1987, 68, 37.
40. Ratner, M.; Shriver, D. F. *Chem Rev* 1988, 88, 109.
41. Williams, M. L.; Landell, R. F.; Ferry, J. D. *J Am Chem Soc* 1955, 77, 3701.
42. Okamoto, Y.; Yeh, T. F., II; Lee, S.; Skotheimk, T. A. L. *Polym Sci Part A Polym Chem* 1993, 31, 2573.